Photoelectron spectroscopy and theoretical study of M(IO3)2− (M = H, Li, Na, K): Structural evolution, optical isomers, and hyperhalogen behavior

Gao-Lei Hou, Miao Miao Wu, Hui Wen, Qiang Sun, Xue-Bin Wang et al.

Citation: J. Chem. Phys. **139**, 044312 (2013); doi: 10.1063/1.4816525
View online: http://dx.doi.org/10.1063/1.4816525
View Table of Contents: http://jcp.aip.org/resource/1/JCPSA6/v139/i4
Published by the AIP Publishing LLC.

Photoelectron spectroscopy and theoretical study of $M(IO_3)_2^-$ (M = H, Li, Na, K): Structural evolution, optical isomers, and hyperhalogen behavior

Gao-Lei Hou,[1,2,a)] Miao Miao Wu,[3] Hui Wen,[2,a),b)] Qiang Sun,[4,c)] Xue-Bin Wang,[2,c)] and Wei-Jun Zheng[1,c)]

[1]*Beijing National Laboratory for Molecular Sciences, State Key Laboratory of Molecular Reaction Dynamics, Institute of Chemistry, Chinese Academy of Sciences, Beijing 100190, China*
[2]*Physical Sciences Division, Pacific Northwest National Laboratory, P. O. Box 999, MS K8-88, Richland, Washington 99352, USA*
[3]*Department of Materials Science and Engineering, China University of Mining and Technology (Beijing), Beijing 100083, China*
[4]*Department of Materials Science and Engineering and Center for Applied Physics and Technology, Peking University, Beijing 100871, China*

(Received 10 June 2013; accepted 10 July 2013; published online 31 July 2013)

$H(IO_3)_2^-$ and $M(IO_3)_2^-$ (M = Li, Na, K) anions were successfully produced via electrospray ionization of their corresponding bulk salt solutions, and were characterized by combining negative ion photoelectron spectroscopy and quantum chemical calculations. The experimental vertical detachment energies (VDEs) of $M(IO_3)_2^-$ (M = H, Li, Na, K) are 6.25, 6.57, 6.60, and 6.51 eV, respectively, and they are much higher than that of IO_3^- (4.77 eV). The theoretical calculations show that each of these anions has two energetically degenerate optical isomers. It is found that the structure of $H(IO_3)_2^-$ can be written as $IO_3^-(HIO_3)$, in which the H atom is tightly bound to one of the IO_3^- groups and forms an iodic acid (HIO_3) molecule; while the structures of $M(IO_3)_2^-$ can be written as $(IO_3^-)M^+(IO_3^-)$, in which the alkali metal atoms interact with the two IO_3^- groups almost equally and bridge the two IO_3^- groups via two O atoms of each IO_3^- with the two MOOI planes nearly perpendicular to each other. In addition, the high VDEs of $M(IO_3)_2^-$ (M = Li, Na, K) can be explained by the hyperhalogen behavior of their neutral counterparts. © *2013 AIP Publishing LLC*. [http://dx.doi.org/10.1063/1.4816525]

I. INTRODUCTION

Metal iodates, especially alkali metal iodates (MIO_3, M = Li, Na, K, Rb, Cs), have received extensive interest due to their potential applications in electro-optic and electromechanical materials.[1–5] The crystal structures of the alkali metal iodates have been characterized several decades ago,[6–13] and it is established that the iodate anion forms a pyramid with I as one apex and the I–O bond lengths being around 1.80 Å. Due to the different sizes of the alkali metals, they have different number of coordinated O atoms in the crystals (for example, Li^+ and Na^+ have six oxygen neighbors, K^+ has eight and Rb^+ has twelve), and thus the structures and properties of these crystals are different. Recently, Yang *et al.*[3] synthesized and characterized a series of alkali metal indium iodates and found that the compounds containing Li^+ and Na^+ prefer to form chain structures, while those containing K^+, Rb^+ or Cs^+ all favor spherical structures. They attributed the differences to the different coordination environments of the alkali metal cations resulted from their different sizes and interactions with the iodates. Therefore, a molecular level study of the interactions between the alkali metals and iodates is desirable to understand the related crystal structures and properties.

On the other hand, Jena and co-workers recently proposed the concept of hyperhalogen to name a new class of highly electronegative species based on anion photoelectron spectroscopy and theoretical study of $Au(BO_2)_2^-$[14] and $Cu(BO_2)_2^-$.[15] These hyperhalogen species are derived from the typical superhalogens in the formula of MX_{k+1} proposed by Gutsev and Boldyrev[16,17] by replacing X with superhalogens such as BO_2.[18] Therefore, the electron affinities (EAs) of hyperhalogens are much higher than those of their superhalogen building blocks. Further theoretical calculations on high EA species suggested that $Na(BO_2)_2$,[19] $Al(BO_2)_4$,[20] $M(BO_2)_{3,4}$ (M = Fe, Mn),[21] $Na(BF_4)_2$,[22] $Mg[Mg(BH_4)_3]_3$[23] and Mn_4Cl_9[24] can also be considered as hyperhalogens.[25] In a recent theoretical study, Anusiewicz[26] predicted that various acidic functional groups (ClO_4, ClO_3, NO_3, HSO_4, etc.) are capable of forming superhalogen anions, for example, $Na(ClO_3)_2^-$ is such an anion with a theoretical vertical detachment energy (VDE) of 6.65 eV. Since IO_3 is a superhalogen with an EA of 4.70 eV,[27] which is higher than that of ClO_3 (4.25 eV),[28] it would be interesting to investigate that whether the series of $M(IO_3)_2^-$ (M = Li, Na, K) using IO_3^- as ligands can be regarded as superhalogen or even hyperhalogen anions?

Motivated by the importance of alkali iodates in material sciences and the search of novel high EA species, we present

a)Visiting students supported by PNNL alternate sponsored fellowship.
b)Permanent address: Laboratory of Atmospheric Physical Chemistry, Hefei Institutes of Physical Sciences, Chinese Academy of Sciences (CAS), Hefei, Anhui 230031, China.
c)Electronic addresses: xuebin.wang@pnnl.gov; zhengwj@iccas.ac.cn; and sunqiang@pku.edu.cn

here a joint negative ion photoelectron spectroscopy (PES) and theoretical study on the geometric and electronic structures of $M(IO_3)_2^-$ (M = H, Li, Na, K).

II. EXPERIMENTAL AND THEORETICAL METHODS

A. Experimental details

The experiments were carried out using a low-temperature electrospray ionization (ESI)-PES apparatus described in a previous publication.[29] A key feature of this apparatus is a 3D cryogenically controlled ion trap that is used for ion accumulation and cooling. Briefly, the desired $M(IO_3)_2^-$ (M = Li, Na, K) anions were produced via electrospraying $\sim 10^{-4}$ M solution of the corresponding MIO_3 salt dissolved in a mixture of acetonitrile/water solvent (3/1 volume ratio), and $H(IO_3)_2^-$ was generated by using $KH(IO_3)_2$ salt. The produced anions from ESI source were guided by two RF-only quadrupole ion guides, and directed by a 90° bender into the temperature controlled Paul trap, where they were accumulated and underwent thermalizing collisions with 0.1 mTorr buffer gas (20% H_2 seeded in He). It has been demonstrated that very cold ions can be created in this manner. After being trapped and cooled at 20 K for 20–100 ms period, the ions were pulsed into the extraction zone of a time-of-flight (TOF) mass spectrometer at a 10 Hz repetition rate.

For each PES experiment, $M(IO_3)_2^-$ anions were mass-selected and decelerated before being interacted with 157 nm photons (7.867 eV) from an F_2 laser in the photodetachment zone of a magnetic bottle photoelectron analyzer. The laser was operated at a 20 Hz repetition rate with the ion beam off at alternating laser shots affording shot-to-shot background subtraction. Photoelectrons were collected at nearly 100% efficiency by the magnetic bottle and analyzed in a 5.2 m long electron flight tube. TOF photoelectron spectra were recorded and converted to kinetic energy spectra calibrated by the known spectra of I^- and $Cu(CN)_2^-$. The electron binding energy spectra were obtained by subtracting the kinetic energy spectra from the detachment photon energy. The electron energy resolution was about 2% (i.e., 20 meV for electrons with 1 eV kinetic energy).

B. Theoretical methods

The calculations were performed using GAUSSIAN 09 program package.[30] The geometric structures were optimized with density functional theory (DFT) using B3LYP exchange-correlation hybrid functional.[31] The Pople's all electron basis set 6-311++G(3df, 3pd)[32] was used for H, Li, Na, K, Cl, and O, and the Stuttgart–Köln MCDHF RSC effective core potential (ECP, 28 core electrons) basis set aug-cc-pVTZ-PP[33] obtained from the EMSL basis set exchange[34] was used for I. The optimizations were performed without any symmetry constraint. To make sure the optimized structures correspond to the real minima on the potential energy surfaces, harmonic vibrational frequencies have been calculated and no imaginary frequencies were found. We tested our theoretical method by comparing our results on $Na(ClO_3)_2^-$ with that reported by Anusiewicz[26] at MP2 level of theory, as well as the optimized MIO_3 geometries with the corresponding crystal structures (Figure S1 in the supplementary material).[35] The natural bond orbital (NBO) analysis was conducted to investigate the nature of bonding in the studied species. The theoretical VDEs were calculated as the energy differences between the neutrals and anions both at the geometries of the anionic species. The theoretical adiabatic detachment energies (ADEs) were calculated as the energy differences between the neutrals and the anions with the neutral structures relaxed to the nearest local minima using the geometries of the corresponding anions as initial structures. All ADEs have been corrected by zero-point vibrational energies.

To provide more reliable VDEs of these species and to justify the reliability of the B3LYP hybrid functional used in this work, more accurate treatment and direct calculations of the electron binding energies (EBEs) based on the outer valence Green function (OVGF) method were also performed.[36–40] This method has been previously shown to provide an excellent agreement between the theoretical and experimental VDEs on a variety of superhalogen anions.[41–44] Since the OVGF approximation is valid only for the outer valence ionizations for which the pole strengths (PSs) are larger than 0.80–0.85,[45] this method is verified to be useful by confirming that all the PSs studied in this work are sufficiently large (*vide infra*). The OVGF calculations were performed on the optimized structures obtained by B3LYP functional and the basis sets used for OVGF are the same as those used for B3LYP.

III. EXPERIMENTAL RESULTS

Figure 1 presents the low temperature (20 K) photoelectron spectra of $M(IO_3)_2^-$ (M = H, Li, Na, K) at 157 nm. Generally, all spectra show significantly higher EBEs than that of IO_3^- by ~1.3 eV for $H(IO_3)_2^-$ and ~1.6 eV for $M(IO_3)_2^-$ (M = Li, Na, K), respectively. Since no vibrational structures are resolved in the threshold region, the ADE is estimated for each species by drawing a straight line along the fast rising edge of the ground state transition, and adding the instrumental resolution to the crossing point with the binding energy axis. The relatively sharp rising onsets in all spectra suggest minor anion-neutral geometric changes after electron photodetachment, which will be confirmed by the theoretical calculations in the following parts. The VDEs of the $M(IO_3)_2^-$ anions are estimated from each respective spectral feature maximum and are summarized in Table I.

The 157 nm spectra of $H(IO_3)_2^-$ and $Li(IO_3)_2^-$ both exhibit two discernible and quite similar spectral features (X & A). However, the features of $Li(IO_3)_2^-$ are relatively narrower and the ADE is surprisingly higher by ~0.37 eV than that of $H(IO_3)_2^-$. Likewise, the spectra of $Na(IO_3)_2^-$ and $K(IO_3)_2^-$ are also very similar with much better resolved spectral features. One more feature (B) is observed near the 157 nm photon energy limit for $K(IO_3)_2^-$.

It is interesting to note that there is a notable EBE increase from $H(IO_3)_2^-$ to $Li(IO_3)_2^-$, and $Na(IO_3)_2^-$ has the largest EBE among these species despite that the differences among $M(IO_3)_2^-$ (M = Li, Na, K) are quite small. In previous studies, it was usually found that the EBE decreases

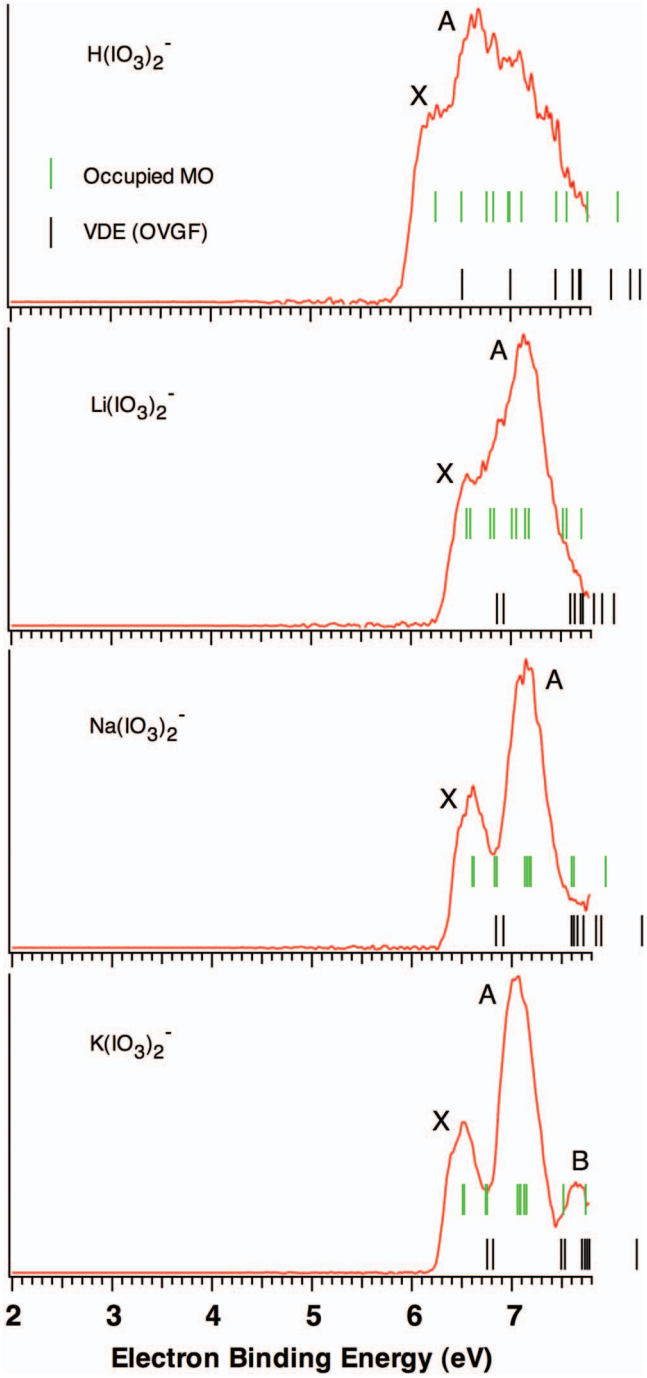

FIG. 1. Low temperature (20 K) photoelectron spectra of $M(IO_3)_2^-$ (M = H, Li, Na, K) at 157 nm. The simulated stick DOS spectra and the OVGF calculated VDEs of the most stable structures of $M(IO_3)_2^-$ (M = H, Li, Na, K) are indicated in green and black vertical lines, respectively.

from Li to Na to K with the increased size of the alkali metal in MX_2^- (M = Li, Na, K; X = F, Cl, Br, I).[35,41,46–48] The finding that $Na(IO_3)_2^-$ has the largest EBE among $M(IO_3)_2^-$ probably can be traced back to the size matching effect of the alkali metals on the cation-anion interactions as observed by Yang *et al.*[3] in alkali metal indium iodates and by Murdachaew *et al.*[49] in the study of M^+ (M = Li, Na, K) ion specific interactions with dicarboxylate dianions. Based on the spectral similarities and differences of these species, significant changes of the interactions between the cation and the two IO_3^- groups are expected when the cation changes from H to different alkali metals.

IV. THEORETICAL RESULTS AND DISCUSSIONS

A. Theoretical results

Electronic structure calculations were performed to obtain the geometric structures of these anions and their corresponding neutrals, the theoretical VDEs and ADEs, and the chemical bonding properties. The most stable geometries of the $M(IO_3)_2^-$ (M = H, Li, Na, K) anions and their corresponding neutrals are presented in Figure 2. It is found that the IO_3^- moiety retains its pyramid configuration in all the anions and neutrals, except that the bonded I–O(–M) bond is slightly longer and the unbonded I–O bond is slightly shorter in the anions compared to the I–O bonds in the isolated IO_3^- (1.829 Å). However, all these bond lengths are in line with the crystal structure measurements.

We also calculated the density of states (DOS) spectra of the most stable structures to compare with the experimental spectra based on theoretically generalized Koopmans' theorem,[50] in which the observed spectral features can be viewed as originating from an electron removal from a specific occupied orbital of the anion. The simulated spectra are obtained by setting the highest occupied molecular orbital (HOMO) transition of the anions as the first experimental VDE, and shifting the deeper orbitals' transitions by the orbital energy differences relative to the HOMO.[51] Here it should be pointed out that in comparison of the simulated DOS spectra with the experimental spectra, the important part is how well the electron binding energies correspond to spectral features and not the relative intensities, so we only plotted out the stick DOS spectra, which are shown in green vertical lines in Figure 1, instead of the fitted DOS spectra.[51] The qualitative DOS spectra based on Koopmans' approximation are compared with the direct OVGF calculations (black vertical lines in Figure 1). Consistent spectral pattern is generally found for each species using both methods, despite the fact that some final excited states at higher energies derived from removal of electrons from close-lying MOs in the anions have different ordering (Table S2 in the supplementary material).[35]

1. $H(IO_3)_2^-$ and $H(IO_3)_2$

As shown in Figure 2, two energetically degenerate optical isomers were found for $H(IO_3)_2^-$, as denoted by H-a and H-b. From the bond lengths, it can be seen that in this ion one IO_3^- connects the HIO_3 part via a strong O–H · · · O hydrogen bond, and the IO_3^- and the HIO_3 parts are only slightly affected by each other compared to the optimized IO_3^- and HIO_3 at the same level of theory (Figure S1 in the supplementary material).[35] Therefore, the $H(IO_3)_2^-$ anion actually should be written as $IO_3^-(HIO_3)$. The NBO charge analysis (Figure S3 in the supplementary material)[35] shows that the charge on IO_3^- is about −0.91 *e* and that on HIO_3 part is only about −0.09 *e*, in agreement with the structure of $IO_3^-(HIO_3)$. Further analysis of the NBO charge indicates that from the neutral $H(IO_3)_2$ to the anion, the H atom only

TABLE I. Experimental and theoretical adiabatic (ADE) and vertical (VDE) detachment energies of $M(IO_3)_2^-$ (M = H, Li, Na, K). The binding energies for $M(IO_3)_2^-$ with respect to dissociation into MIO_3 and IO_3^- are also given. All energies are in eV.

		ADE		VDE			
					Theo.		
$M(IO_3)_2^-$		Expt.[a]	Theo.	Expt.[a]	B3LYP	OVGF[b]	Binding energy[c]
H	X	5.95(8)	(a) 5.39	6.25(10)	5.77	6.53 (0.917)	1.37
			(b) 5.39		5.77	6.53 (0.917)	
	A			6.68(10)			
Li	X	6.32(8)	(a) 5.76 (5.31)	6.57(10)	5.94	6.88 (0.921)	1.82
			(b) 5.34		5.83	6.88 (0.921)	
	A			7.13(8)			
Na	X	6.35(8)	(a) 5.71	6.60(8)	5.77	6.86 (0.923)	1.84
			(b) 5.72		5.77	6.86 (0.923)	
	A			7.14(8)			
K	X	6.30(8)	(a) 5.59	6.51(8)	5.76	6.77 (0.924)	1.62
			(b) 5.59		5.76	6.77 (0.924)	
	A			7.04(8)			
	B			7.65(8)			

[a]The numbers in the parentheses represent the experimental uncertainty in the last digits.
[b]The numbers in the parentheses indicate the calculated pole strengths (PSs) for the corresponding states. All the PSs are larger than 0.80–0.85.
[c]The binding energies are calculated using the equation $BE = E(MIO_3) + E[(IO_3)^-] - E[M(IO_3)_2^-]$, all energies have been corrected by zero-point energy.

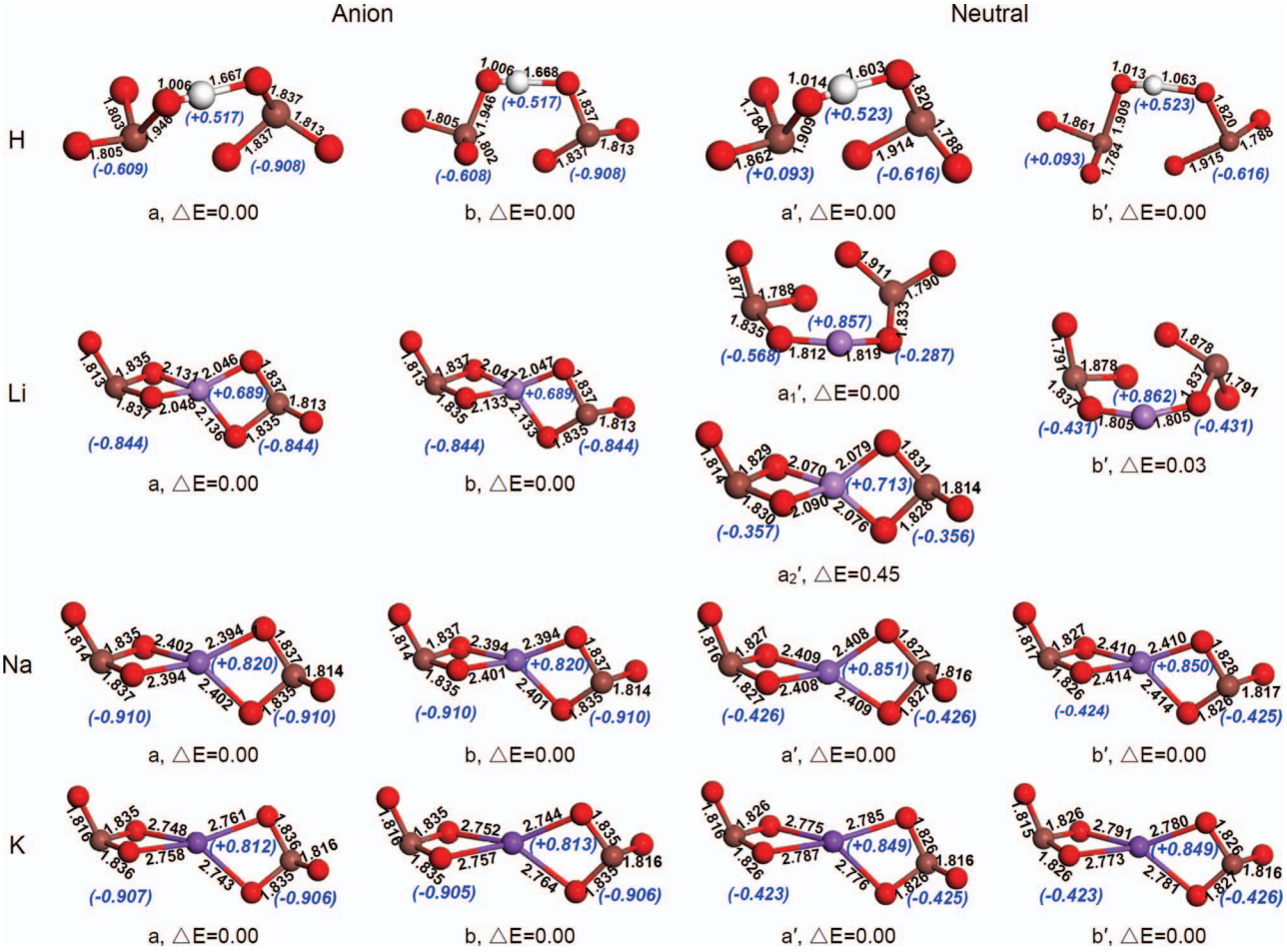

FIG. 2. The most stable structures of $M(IO_3)_2^-$ (M = H, Li, Na, K) anions and their corresponding neutrals. Two energetically degenerate optical isomers for each anion are given. Selected bond lengths (in Å), the NBO charge on M atom and IO_3^- moieties (in italic), and relative energies (in eV) are indicated.

obtained about −0.006 *e*, while the IO_3^- group in the HIO_3 part obtained about −0.70 *e* and the other IO_3^- about −0.29 *e*. The molecular orbital (MO) analysis (Figure S4 in the supplementary material)[35] reveals that the HOMO of $H(IO_3)_2^-$ consists almost purely of the combination of O(p) and I(s) of the IO_3^- groups, and the HOMO displays a non-bonding character between the central H atom and the ligands. Comparing the neutral $H(IO_3)_2$ to the anion, there is only minor geometric change with O–H being longer by ∼0.007 Å and O · · · H being ∼0.064 Å shorter in the neutral, consistent with the fast rising onset of the spectrum. The change can be attributed to the removal of the extra electron which has decreased the electrostatic interaction between the H atom and the IO_3^- group in the HIO_3 part. The calculated ADE and VDE using B3LYP functional are 5.39 and 5.77 eV, respectively, both lower than the corresponding experimental values by about 0.6 eV. It has been shown previously that B3LYP usually underestimated the ADE and VDE of other superhalogen anions.[43] The simulated stick DOS spectra agree well with the experimental spectrum, providing considerable credence for the obtained geometric structures of $H(IO_3)_2^-$. The VDE of $H(IO_3)_2^-$ (both a and b) predicted by the OVGF method is 6.53 eV, in a much better agreement with the experimental value of 6.25 eV.

2. $Li(IO_3)_2^-$ and $Li(IO_3)_2$

Similar to $H(IO_3)_2^-$, two energetically degenerate optical isomers were also found for $Li(IO_3)_2^-$ anions and are shown in Figure 2. For the neutrals, apart from two optical isomers whose structures are different from their corresponding anions, we also found a local minimum Li-a_2', which is similar to its anionic counterpart but about 0.42–0.45 eV higher in energy than the other two isomers Li-a_1' and Li-b′. In both isomers Li-a_1' and Li-b′, the two IO_3^- groups stay on one side of O–Li–O bond and surprisingly have much shorter Li–O bond lengths (∼1.805–1.819 Å in the neutral vs ∼2.046–2.133 Å in the anion). The NBO charge analysis shows that the charges on the Li atom in the neutral and the anion are about +0.86 *e* and +0.69 *e*, respectively, while those on the nearest O atoms in the neutral and the anion are ∼−1.15 *e* and ∼−1.09 *e*, respectively. Thus, the electrostatic interaction between the Li atom and the nearest O atoms is larger and consequently the Li–O bond length is shorter in the neutral. From the NBO charge analysis, it can also be seen that the extra electron has been almost delocalized on the two IO_3^- groups with each one obtaining about −0.41 *e* from neutral to anion. The HOMO of $Li(IO_3)_2^-$ clearly shows a non-bonding character between the central Li atom and the two IO_3^- groups, and thus the extra electron can be highly stabilized. The theoretical ADEs and VDEs at B3LYP level are 5.31 (a_1')/5.76 (a_2') and 5.94 eV for Li-a, and 5.34 and 5.83 eV for Li-b, respectively. Regarding the fast rising onset of the experimental spectrum of $Li(IO_3)_2^-$, the final state of the electron photodetachment probably will be Li-a_2'. The calculated ADE and VDE are again lower than the corresponding experimental values by about 0.6 eV as found in the case of $H(IO_3)_2^-$. The simulated stick DOS spectra are in agreement with the experiments, confirming the validity of the optimized geometric structures for $Li(IO_3)_2^-$. In addition, the VDE of $Li(IO_3)_2^-$ (a and b) at the OVGF level is 6.88 eV, in good agreement with the experimental value of 6.57 eV and excellently reproducing the experimental EBE increase from $H(IO_3)_2^-$ to $Li(IO_3)_2^-$.

3. $Na(IO_3)_2^-$ and $Na(IO_3)_2$

Figure 2 shows two energetically degenerate optical isomers for $Na(IO_3)_2^-$ and its corresponding neutrals, where the central Na atom bridges equally the two identical IO_3^- groups. The anionic structures and the corresponding neutrals are very similar except that the Na–O bonds are slightly longer and the I–O(–Na) bonds are slightly shorter in the neutrals. The NBO charge analysis indicates that the extra electron has been delocalized over the two IO_3^- groups with about −0.48 *e* on each from neutral to anion. The HOMO of $Na(IO_3)_2^-$ shows the same non-bonding character as in $Li(IO_3)_2^-$. The calculated ADE and VDE using B3LYP functional are 5.71 and 5.77 eV, respectively, lower than the corresponding experimental values by about 0.6–0.8 eV. The simulated spectra based on the geometries of $Na(IO_3)_2^-$ anion are in good agreement with the experimental spectrum. The OVGF calculated VDE is 6.86 eV and agrees well with the experimental value of 6.60 eV.

4. $K(IO_3)_2^-$ and $K(IO_3)_2$

Not surprisingly, two energetically degenerate optical isomers were also found for $K(IO_3)_2^-$ anions and their neutrals. Generally, they show the similar anion-neutral geometric changes as $Na(IO_3)_2^{-/0}$. The NBO charge analysis indicates that the extra electron has been delocalized over the two IO_3^- groups and each one obtains about −0.48 *e*. The HOMO of $K(IO_3)_2^-$ is also similar to those of $Li(IO_3)_2^-$ and $Na(IO_3)_2^-$. The calculated ADE and VDE using B3LYP functional are 5.59 and 5.76 eV, respectively, lower than the corresponding experimental values by about 0.7 eV. The simulated stick DOS spectra based on the geometries of $K(IO_3)_2^-$ anion agree well with the experimental spectrum, and the VDE of 6.77 eV obtained by the OVGF calculations is in good agreement with the experimental value of 6.51 eV.

B. Discussion

1. Structural evolution and optical isomers of $M(IO_3)_2^-$

From the above analysis on the structures of $M(IO_3)_2^-$ (M = H, Li, Na, K), it is suggested that $H(IO_3)_2^-$ should be considered as a IO_3^- ion solvated by an iodic acid (HIO_3) molecule, $IO_3^-(HIO_3)$. In this structure, HIO_3 behaves like a solvent, similar to our previously reported mono-water solvated IO_3^- complex of $IO_3^-(H_2O)$.[52] However, the hydrogen bond in $IO_3^-(HIO_3)$ is much stronger than those in $IO_3^-(H_2O)$, which may explain why the VDE of $IO_3^-(HIO_3)$ (6.25 eV) is much higher than that of $IO_3^-(H_2O)$ (5.32 eV). In contrast to $IO_3^-(HIO_3)$, the other three anions $M(IO_3)_2^-$ (M = Li, Na, K) should be considered as $(IO_3^-)M^+(IO_3^-)$, where the central metal atom bridges two IO_3^- groups via two M–O bonds for each IO_3^-, and the two MOOI planes

of each structure are nearly perpendicular to each other. In these complexes, the average M–O bond lengths are different and they are about 2.13, 2.39, 2.75 Å for M = Li, Na, K, respectively. This is most likely due to the size effect of the alkali metal atoms (for example, the ionic radii[53] of Li, Na, K atom are 0.68, 0.97, and 1.33 Å, respectively). The bonding difference between the structures of $H(IO_3)_2^-$ and $M(IO_3)_2^-$ (M = Li, Na, K) is due to the fact that H atom is too small to accommodate the four-coordinate bonding as observed in the latter cases, resulting in covalently bound to one of the two IO_3^- ions to form an iodic acid molecule in the former instance.

All these anions have two energetically degenerate optical isomers and both isomers are observed by the experiments. Thus, we postulate that optical isomerism may be common in this $M(XO_3)_2^-$ (M = alkali metal; X = halide) type of ions. To test this idea, we conducted structures search on $Na(ClO_3)_2^-$, which has been reported previously by Anusiewicz[26] and indeed found two optical isomers degenerate in energy for $Na(ClO_3)_2^-$. In the two isomers, one is similar to the structure reported by Anusiewicz and one is its optical isomer (Figure S2 in the supplementary material).[35] Both of them have VDEs of 5.74 eV at B3LYP level, and their VDEs obtained by OVGF calculations are both 6.63 eV, close to the value of 6.65 eV reported by Anusiewicz using OVGF//MP2 method. In addition, as these anions were produced via electrospray ionization of the corresponding salt solutions, the optical isomers may exist in the solutions before their transfer into the gas phase, and their existence in the solid phase may also be possible, which may relate to the unique optical properties of the corresponding MIO_3 crystals.

2. Hyperhalogen behavior of $M(IO_3)_2$

Considering the typical superhalogen formula MX_{k+1},[16,17] and the fact that IO_3 is a superhalogen, $M(IO_3)_2$ (M = Li, Na, K) probably can be regarded as MX_2 (X = IO_3) type superhalogens or hyperhalogens, similar to the case of $M(BO_2)_2$ (M = Au, Cu). From the NBO charge and MO analysis, it can be seen that the extra electron has been almost delocalized on the two IO_3^- ligands, ranging from about −0.41 *e* to about −0.48 *e* on each, and the HOMOs of these anions all have a significant non-bonding character. The highly delocalized extra electrons and the non-bonding HOMOs lead to very high VDEs for the anions and very high EAs for the corresponding neutrals. Interestingly, the VDEs of these species are higher than that of IO_3^- by about 1.6 eV and even higher than those of MX_2^- (M = Li, Na, K; X = F, Cl, Br, I) (Table S1 in the supplementary material).[35] Further calculations on the binding energies of IO_3^- to MIO_3 (Table I) for these anionic species provide values of 1.82, 1.84, and 1.62 eV for $Li(IO_3)_2^-$, $Na(IO_3)_2^-$ and $K(IO_3)_2^-$, respectively, indicating that these anions have high stability toward dissociation, in agreement with the abundant intensity of $M(IO_3)_2^-$ observed in the mass spectra. Therefore, these species can be considered as hyperhalogen anions and their neutrals are hyperhalogens. In contrast, the high VDE of $H(IO_3)_2^-$ can be attributed to the solvation effect induced by the formation of the strong O–H · · · O hydrogen bond, and its calculated binding energy is 1.37 eV, about 0.3–0.5 eV lower than those for its alkali metal congeners.

V. CONCLUSION

We investigated $H(IO_3)_2^-$ and $M(IO_3)_2^-$ (M = Li, Na, K) anions using negative ion photoelectron spectroscopy, density functional calculations and *ab initio* outer valence Green function calculations. It is found that all these anions have two energetically degenerate optical isomers, suggesting that the optical isomerism may be common in $M(XO_3)_2^-$ (M = alkali metal; X = halide) type of anions. The structure of $H(IO_3)_2^-$ can be recognized as a IO_3^- ion solvated by a HIO_3 molecule and there is a strong O–H · · · O hydrogen bond between IO_3^- and HIO_3. This structure configuration is in contrast to its alkali metal congeners, whose structures can be written as $(IO_3^-)M^+(IO_3^-)$ with M^+ bridging two IO_3^- groups. The subtle difference among the structures of $M(IO_3)_2^-$ (M = Li, Na, K) is due to the size effect of the alkali metal atoms. In addition, the high VDEs of $M(IO_3)_2^-$ (M = Li, Na, K) anions (higher than that of IO_3^-) measured from photoelectron spectroscopy experiments can be explained by the hyperhalogen behavior of their corresponding neutrals, while the high VDE of $H(IO_3)_2^-$ can be attributed to the solvation effect induced by forming a strong hydrogen bond.

ACKNOWLEDGMENTS

The experimental work done at Richland was supported by the Division of Chemical Sciences, Geosciences, and Biosciences, Office of Basic Energy Sciences, U. S. Department of Energy (DOE), and was performed using EMSL, a national scientific user facility sponsored by DOE's Office of Biological and Environmental Research and located at Pacific Northwest National Laboratory, which is operated by Battelle Memorial Institute for the DOE. The theoretical work was partially supported by grants from the Natural Science Foundation of China (Grant No. NSFC-21173007). G.-L.H. thanks Dr. V. G. Zakrzewski (Auburn University) for valuable help on the OVGF calculations. Q.S. and M.M.W. thank the crew of the Center for Computational Materials Science, the Institute for Materials Research, Tohoku University, Japan for their continuous support. The theoretical work was conducted using the resource of the HITACH SR11000 supercomputing facility, as well as the ScGrid and Deepcomp7000 of the Supercomputing Center, Computer Network Information Center of Chinese Academy of Sciences.

[1] J. G. Bergman, J. Appl. Phys. **40**, 2860 (1969).
[2] S. K. Kurtz, Appl. Phys. Lett. **12**, 186 (1968).
[3] B.-P. Yang, C.-F. Sun, C.-L. Hu, and J.-G. Mao, Dalton Trans. **40**, 1055 (2011).
[4] M. S. Wickleder, Chem. Rev. **102**, 2011 (2002).
[5] K. M. Ok, E. O. Chi, and P. S. Halasyamani, Chem. Soc. Rev. **35**, 710 (2006).
[6] I. Naray-Szabo and A. Kalman, Acta Crystallogr. **14**, 791 (1961).
[7] M. T. Rogers and L. Helmholz, J. Am. Chem. Soc. **63**, 278 (1941).
[8] G. Kunze and S. A. Hamid, Acta Crystallogr. **B33**, 2795 (1977).
[9] H. Kasatani, S. Aoyagi, Y. Kuroiwa, K. Yagi, R. Katayama, and H. Terauchi, Nucl. Instrum. Methods Phys. Res. B **199**, 49 (2003).
[10] C. Svensson, J. Chem. Phys. **78**, 7343 (1983).

[11]I. Naray-Szabo and D. J. Neugebauer, J. Am. Chem. Soc. **69**, 1280 (1947).
[12]C. Svensson and K. Stahl, J. Solid State Chem. **77**, 112 (1988).
[13]N. W. Alcock, Acta Crystallogr., Sect. B: Struct. Sci. **28**, 2783 (1972).
[14]M. Willis, M. Götz, A. K. Kandalam, G. F. Ganteför, and P. Jena, Angew. Chem. Int. Ed. **49**, 8966 (2010).
[15]Y. Feng, H.-G. Xu, W. Zheng, H. Zhao, A. K. Kandalam, and P. Jena, J. Chem. Phys. **134**, 094309 (2011).
[16]G. L. Gutsev and A. I. Boldyrev, Chem. Phys. **56**, 277 (1981).
[17]G. L. Gutsev and A. I. Boldyrev, Chem. Phys. Lett. **108**, 250 (1984).
[18]H.-J. Zhai, L.-M. Wang, S.-D. Li, and L.-S. Wang, J. Phys. Chem. A **111**, 1030 (2007).
[19]K. Pradhan and P. Jena, J. Chem. Phys. **135**, 144305 (2011).
[20]G. L. Gutsev, C. A. Weatherford, L. E. Johnson, and P. Jena, J. Comput. Chem. **33**, 416 (2012).
[21]P. Koirala, K. Pradhan, A. K. Kandalam, and P. Jena, J. Phys. Chem. A **117**, 1310 (2013).
[22]C. Paduani and P. Jena, J. Phys. Chem. A **116**, 1469 (2012).
[23]C. Paduani and P. Jena, Chem. Phys. Lett. **556**, 173 (2013).
[24]Y. Li, S. Zhang, Q. Wang, and P. Jena, J. Chem. Phys. **138**, 054309 (2013).
[25]P. Jena, Chem. Phys. Lett. **4**, 1432 (2013).
[26]I. Anusiewicz, J. Phys. Chem. A **113**, 11429 (2009).
[27]H. Wen, G.-L. Hou, W. Huang, N. Govind, and X.-B. Wang, J. Chem. Phys. **135**, 184309 (2011).
[28]X.-B. Wang and L.-S. Wang, J. Chem. Phys. **113**, 10928 (2000).
[29]X.-B. Wang and L.-S. Wang, Rev. Sci. Instrum. **79**, 073108 (2008).
[30]A. M. Simas, R. O. Freire, and G. B. Rocha, Lect. Notes Comput. Sci. **4488**, 312 (2007).
[31]A. M. Simas, R. O. Freire, and G. B. Rocha, J. Organomet. Chem. **693** (10), 1952 (2008).
[32]R. Krishnan, J. S. Binkley, R. Seeger, and J. A. Pople, J. Chem. Phys. **72**, 650 (1980).
[33]K. A. Peterson, D. Figgen, E. Goll, H. Stoll, and M. Dolg, J. Chem. Phys. **119**, 11113 (2003).
[34]N. B. da Costa, R. O. Freire, A. M. Simas, and G. B. Rocha, J. Phys. Chem. A **111**(23), 5015 (2007).
[35]See supplementary material at http://dx.doi.org/10.1063/1.4816525 for optimized structures of IO_3^-, MIO_3 (M = H, Li, Na, K) (Figure S1), and $Na(ClO_3)_2^-$ and its corresponding neutral (Figure S2), MO, and NBO charge analysis (Figures S3 and S4), reported ADEs and VDEs of MX_2^- superhalogen anions (Table S1) and the correspondence of the orbital energies between the Koopmans' theorem, and outer valence approximation (Table S2).
[36]V. G. Zakrzewski, J. V. Ortiz, J. A. Nichols, D. Heryadi, D. L. Yeager, and J. T. Golab, Int. J. Quantum Chem. **60**, 29 (1996).
[37]J. V. Ortiz, J. Chem. Phys. **89**, 6348 (1988).
[38]L. S. Cederbaum, J. Phys. B **8**, 290 (1975).
[39]V. G. Zakrzewski and J. V. Ortiz, Int. J. Quantum Chem. **53**, 583 (1995).
[40]V. G. Zakrzewski and J. V. Ortiz, Int. J. Quantum Chem., Quantum Chem. Symp. **52**, 23 (1994).
[41]X.-B. Wang, C.-F. Ding, L.-S. Wang, A. I. Boldyrev, and J. Simons, J. Chem. Phys. **110**, 4763 (1999).
[42]A. N. Alexandrova, A. I. Boldyrev, Y.-J. Fu, X. Yang, X.-B. Wang, and L.-S. Wang, J. Chem. Phys. **121**, 5709 (2004).
[43]B. M. Elliott, E. Koyle, A. I. Boldyrev, X.-B. Wang, and L.-S. Wang, J. Phys. Chem. A **109**, 11560 (2005).
[44]S. Smuczyńska and P. Skurski, Chem. Phys. Lett. **452**, 44 (2008).
[45]V. G. Zakrzewski, O. Dolgounitcheva, and J. V. Ortiz, J. Chem. Phys. **105**, 5872 (1996).
[46]M. K. Scheller and L. S. Cederbaum, J. Chem. Phys. **99**, 441 (1993).
[47]G. L. Gutsev, R. J. Bartlett, A. I. Boldyrev, and J. Simons, J. Chem. Phys. **107**, 3867 (1997).
[48]G. L. Gutsev, P. Jena, and R. J. Bartlett, J. Chem. Phys. **111**, 504 (1999).
[49]G. Murdachaew, M. Valiev, S. M. Kathmann, and X.-B. Wang, J. Phys. Chem. A **116**, 2055 (2012).
[50]D. J. Tozer and N. C. Handy, J. Chem. Phys. **108**, 2545 (1998).
[51]H. Hakkinen, B. Yoon, U. Landman, X. Li, H. J. Zhai, and L.-S. Wang, J. Phys. Chem. A **107**, 6168 (2003).
[52]H. Wen, G.-L. Hou, S. M. Kathmann, M. Valiev, and X.-B. Wang, J. Chem. Phys. **138**, 031101 (2013).
[53]R. D. Shannon and C. T. Prewitt, Acta Crystallogr. **B25**, 925 (1969).